

RAQUEL R. M. BARROS¹, ARTHUR B. NOVAES Jr.², VULA PAPALEXIOU³, SÉRGIO L. S. SOUZA², MÁRIO TABA Jr.², DANIELA B. PALIOTO², MÁRCIO F. M. GRISI²

¹ Graduate student of Periodontology, Department of Bucco-Maxillo-Facial Surgery and Traumatology and Periodontology, School of Dentistry of Ribeirão Preto, University of São Paulo, Brazil

² Professor of Periodontology, Department of Bucco-Maxillo-Facial Surgery and Traumatology and Periodontology, School of Dentistry of Ribeirão Preto, University of São Paulo, Brazil

³ Professor of Periodontology, Center of Biologic and Health Science, School of Dentistry, Catholic Pontifical University, PR, Brazil

The dynamics of bone remodeling around biofunctionalized implant surfaces. A fluorescence analysis in a dog model

ABSTRACT

Background The aim of this study was to evaluate the bone remodeling around different implant surfaces by a fluorescence analysis.

Materials and Methods The mandibular bilateral premolars of 8 dogs were extracted and after 12 weeks each dog received 6 implants. The 4 experimental groups were constituted of implants with the same microstructured topography with or without some concentration of a bioactive peptide. During the healing period of 2 months, polychromatic fluorescence labeling was performed to investigate the dynamics of bone remodeling around the different implant surfaces. The bone markers were administered on the third day after implant placement and then after 1, 2, 4 and 6 weeks.

Results New bone formation was determined histomorphometrically by bone markers quantifications adjacent and distant to the implants surfaces. In general, the intra-group analysis showed a pattern of fluorochrome incorporation among the different groups. However, the comparison between the groups revealed a statistically significant difference in favor of the microstructured surface modified with a "low concentration of a bioactive peptide" at the adjacent area in the 4-week period only ($p < 0.001$). Additionally at 3-day and at 6-week periods this group also achieved numerically superior values of fluorochrome incorporation.

Conclusion Bone remodeling is an active process resulting from the alternation of resorptive and formative activities. There is a similar pattern of bone remodeling among the microstructured surfaces, biofunctionalized or not; however the addition of an adhesive peptide in "low concentration" favored the bone formation adjacent to the implants when compared to the other surfaces during the period evaluated.

KEYWORDS Animal experimentation; Bone remodeling; Dental implants; Fluorescence

INTRODUCTION

Upon implantation, the surfaces of synthetic materials invariably become coated with a thin proteinaceous film (1). Protein orientation will be dependent on the particular binding surface, and various surface characteristics may modify their biologic activity first in relation to cell attachment and in sequence in bone apposition (2). When dealing with titanium, which is a commonly used biocompatible metal, the formation of a superficial oxide layer is expected and the interaction of cells with this layer is mediated by the existent surface proteins, the extracellular matrix proteins (2).

A common theme in the engineering of cell and tissue behavior at device surfaces is to modify the material to selectively interact with a specific cell type through biomolecular recognition events. Typically, peptides containing the cell-binding domains found in the extracellular matrix proteins are immobilized on the material to promote cell adhesion via ligand-receptor interactions (3, 4).

According to the parameters used to evaluate osseointegration, very good results have been achieved with microstructured implant surfaces provided by the grit-blasting/acid-etching process. However, the surface topography is not the only surface characteristic that influences the bone

apposition around titanium implants. Chemical and biochemical composition of implant surface may also play a crucial role in bone formation around implants, especially when the early stages of this process are considered (1, 5). Based on this, surface functionalization using different peptides, for example, are now being investigated.

Some *in vitro* studies are focusing on the cell recruitment ability onto implant-modified surfaces (6, 7). These surfaces have been obtained through different processes, frequently involving a biofunctionalization with adhesive peptides. Schuler et al. (7) investigated cell adhesion and spreading patterns of epithelial cells, fibroblasts and osteoblasts on a biomimetically modified surface (containing a RGD bioactive peptide sequence), and on smooth and rough titanium surfaces. As control surfaces, bare titanium and bio-inactive surfaces were used. In general, an increase in cell number and more spreading of cells were observed on bioactive substrates (containing RGD) compared to bio-inactive surfaces. More fibroblasts were present on smooth than on rough topographies, whereas for osteoblasts the opposite tendency was observed. Osteoblast attachment and footprint areas increased with increasing RGD-peptide surface density. They concluded that surface topography and (bio) chemistry are key factors in determining cell response to an implant.

Animal studies support the hypothesis that the biofunctionalization of implant surfaces could be an advantageous (8-10). Park et al. (8) evaluated the osseointegration of anodized titanium implants coated with fibroblast growth factor-fibronectin (FGF-FN) fusion protein that were placed in rabbit tibiae. The removal torque values as well as the percentages of bone-implant contact of the test group were better than those found for the implants that were not biofunctionalized. Germanier et al. (10) compared RGD peptide polymer modified implant surfaces with sandblasted and acid-etched implant surfaces placed in the maxillae of miniature pigs, and found that the biofunctionalization may promote enhanced bone apposition during the early stages of bone regeneration.

Fluorescence labeling of bone is a method for bone morphometry that provides an understanding of the chronological history of bone remodeling (11), as well as about the early stages of the establishment of bone-to-implant interface. The process of bone formation initiates with the formation of a non-calcified matrix by the osteoblasts, which will later mineralize as a result of apatite deposition, and during this formation phase fluorochromes can be accumulated. According to Nkenke et al. (12) "during the mineralization process, the fluorescent dyes are incorporated in the front of mineralization by

chelation". By marking different time intervals, the sequential administration of different fluorescent dyes allows to follow the direction and the topographic localization of new bone formation.

The purpose of this study was to analyze, in a dog model using polyfluorochrome sequential labeling, the bone remodeling process around implant surfaces containing a low and a high concentration of a bioactive peptide and also to compare them with other implant surfaces such as a microstructured surface created by a grit-blasting/acid-etching process.

MATERIALS AND METHODS

Implant design and manufacturing

All implants were manufactured from commercially pure titanium following the XiVE design (Dentsply Friadent, Mannheim, Germany) and measured 4.5 mm X 9.5 mm. The implants were characterized by an indentation placed 2.3 mm from the top of the implant with a depth of 0.18 mm and a height of 1.5mm (Fig. 1). In this indentation 4 different coatings were performed constituting the 4 different implant groups A, B, C and D (Table 1). Firstly, the indentations of all 4 groups were lined by the microstructured Friadent plus surface (Dentsply Friadent, Mannheim, Germany) provided by the grit-blasting/acid-etching process.

The biofunctionalization of the implant surface was done by the absorption of a bioactive peptide to nano-crystalline HA coatings. The bioactive peptide could also be described as a sequence of aminoacids related to bone formation; however the detailed composition has not been disclosed by the manufacturer (proprietary processing). Thus, group A was constituted by the microstructured morphology and a "low concentration" of the bioactive peptide/nano-crystalline HA coating, while group D has the same characteristics but a "high concentration" of the bioactive peptide. In group B the implants were lined by the microstructured morphology in conjunction with the nano-crystalline HA coating without the bioactive peptide absorption and, finally, in group C they were prepared only with the Friadent plus surface.

The study was blinded, thus all the professionals involved, from the surgeon to the examiner of the fluorescence images, had no knowledge of the constitution of the groups. The different coatings that characterized the 4 different implant surfaces were only revealed when the fluorescence analysis was finished.

Surgical Procedure

The study protocol was approved by the Institution's

Animal Research Committee and involved 2 surgical interventions that were performed in 8 young adult male mongrel dogs, weighing approximately 12 kg. The animals presented intact maxillas, no general occlusal trauma, and no oral viral or fungal lesions and were in good general health, with no systemic involvement as determined by a veterinarian following clinical examination.

In the first surgery, after sedation the dogs were anesthetized with thiopental iv (1 ml/kg; 20 mg/kg thiopental diluted in 50 ml saline). Subsequently, full-thickness flaps were bilaterally elevated in the area of the first to fourth mandibular premolars. The teeth were sectioned in a buccolingual direction at the bifurcation so that the roots could be individually extracted, without damaging the bony walls, using a periosteal elevator. The flaps were repositioned and sutured with non-absorbable 4-0 sutures.

After a healing period of three months, the animals received 20,000 IU penicillin and streptomycin (1.0 g/10 kg) the night before the second surgeries. This dose provides antibiotic coverage for 4 days, thus another dose was given 4 days later to extend the coverage for 8 days. After repeating the same sedation and anesthesia used in the first surgeries, horizontal crestal incisions were bilaterally performed from the distal region of the canine to the mesial region of the first molar. Three implants were randomly inserted in each side of the mandible of each animal. Thus the locations and sides of the mandibles of the animals were treated with different

sequences of implant groups. A total of 48 implants were used in the experiment, twelve for each group (A, B, C or D). The flaps were sutured with non-absorbable sutures and the implants were left to heal in a submerged position. The animals were maintained on a soft diet for 14 days when the sutures were removed. The healing was evaluated periodically and the remaining teeth were cleaned monthly with ultrasonic points. During the 2-month healing period fluorescence bone markers were administered (13) to observe the degree and extent of new bone formation. On the third day after implant placement, 20 mg calcein green/Kg body weight was administered intravenously (Sigma Chemical Co., St Louis, MO, USA); at first week, 20 mg of red alizarin S/Kg body weight (Sigma); at 2 weeks, 20mg oxytetracyclin HCl/Kg body weight (Sigma); at 4 weeks, 20 mg calcein green/Kg body weight (Sigma); and at 6 weeks, 20 mg calcein blue/Kg body weight (Sigma). All dyes were prepared immediately before use with 2% sodium bicarbonate or saline. After preparation, pH was adjusted to 7.4 and the solution was filtered through a 0.45 µm filter (Schleider & Schuell GmbH, Dassel, Germany). Each dog received a total dose of 3 ml.

Sacrifice and histological processing

The animals were sedated and then sacrificed with an overdose of thiopental eight weeks after implant placement. The hemi-mandibles were removed, dissected and fixed in 4% phosphate-buffered formalin pH 7, for 10 days, and transferred to a solution of 70% ethanol until processing. The specimens were dehydrated in increasing concentrations of alcohol up to 100%, infiltrated and embedded in LR White resin (London Resin Company, Berkshire, England), and hard-sectioned using the technique described by Donath & Breuner (14). The specimens were ground to about 50 µm for fluorescence microscopy (12).



Fig. 1 Implant design. All the implants had the same basic form and topography (grit-blasted/acid-etched), but possessed four different surface coatings performed in the indentations that were placed at 2.3mm from the top with a depth of 0.18mm and a height of 1.5mm.

Group	Implant surface characteristics
A	FRIADENT plus surface morphology + HA coating + "low concentration" bioactive peptide
B	FRIADENT plus surface morphology + HA coating
C	FRIADENT plus surface (grit-blasting/acid-etching process)
D	FRIADENT plus surface morphology + HA coating + "high concentration" bioactive peptide

Table 1 Four experimental implant surface groups

Fluorescence analysis

Fluorescence microscopic images were longitudinally captured from each implant through a video camera Leica DC 300F (Leica Microsystems GmbH, Nussloch, Germany) joined to a stereomicroscope Leica MZFL III (Leica Microsystems GmbH, Nussloch, Germany), using appropriated barrier filters. The filters of wavelengths used were D for oxytetracyclin HCl that has an excitation level between 355-425 nm and A for calcein blue that has an excitation level between 340-380 nm. Considering that the calcein green was used in 2 different times (at 3 days after implant placement and at 4 weeks after implant placement), another images were obtained by the confocal laser scanning microscope (CLSM), which obtains successive images of different planes of the same sample, being able to build three-dimensional images. Once the red alizarin S was administered between the 2 administrations of calcein green, it was possible to distinguish the bone marked by calcein green in the different periods using the images provided by the CLSM. All the images were adjusted and analyzed through the Image J program (National Institutes of Health, Bethesda, EUA) to determine the percentages of bone marked at the indentations. The marked bone was determined within 2 rectangles, one of them within the indentation (II), occupying its total area, and the other outside the indentation (OI) as mirror image of the first. The marked bone measurements evaluated the percentages of fluorescent bone in relation to the total area. A single examiner, with no knowledge if the sections were from groups A, B, C or D made the measurements.

Statistical analysis

All measurements were statistically evaluated using the analysis of variance, ANOVA, with 2 factors (surface treatment and label/time) and Tukey test was used for multiple comparisons among the means. The confidence level was 95%.

RESULTS

First of all it is important to emphasize that the microstructured morphology was not changed due to the surfaces' biofunctionalization process. The FRIADENT plus surface morphology was fully maintained following the application of a thin HA + bioactive peptide coating as seen in the SEM images (Fig. 2).

The analysis under fluorescent microscopy showed intense bone remodeling for all the groups evaluated. The old bone always appeared darker and without labeling (Fig. 3). Alizarin had a red color in a smeared diffuse pattern; clearly evident green bands generally represented calcein green; oxytetracyclin showed thin yellow-green lines and finally calcein blue was characterized by a blue color in a very diffuse pattern (Fig. 3). In many specimens the secondary osteons were demonstrated by the deposition of the labels in a concentric arrangement (Fig. 3, 4). New bone formation was determined histomorphometrically by bone markers quantifications. Sequentially, they represented the healing pattern of each different group. The percentages of newly formed bone inside the indentation (II) adjacent to the implant interface were described in Table 1 and were represented in Figure 5. In addition, the percentages of newly formed bone outside the indentation (OI) and distant from the implant interface are described in Table 3 and in Figure 6.

The comparison of the bone marked found in area II between the groups revealed a statistically significant difference in favor of group A in the 4-week period only ($p < 0.001$), although at 3-day and at 6-week periods group A also achieved numerically superior values of fluorochrome incorporation. The evaluation of the OI area showed quite similar results for all the groups considering all the application periods. There were no statistically significant differences between the groups.

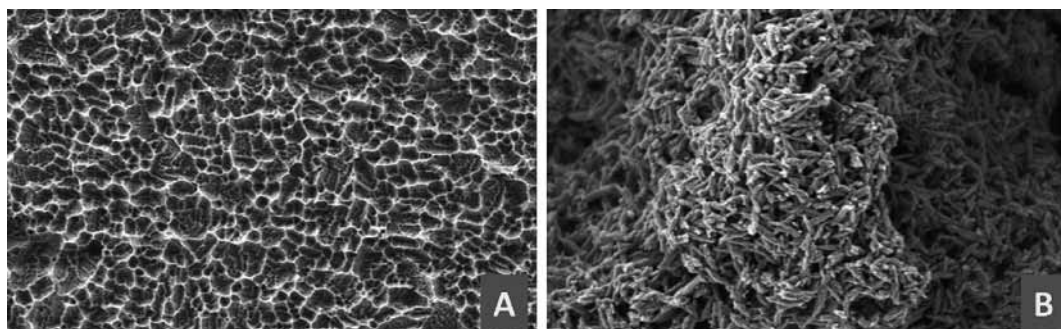


Fig. 2 SEM images. Note the uniform coating not changing the original FRIADENT plus morphology.
(A) FRIADENT plus surface (magnification 1.000x);
(B) FRIADENT plus surface after coating with HA/bioactive peptide (magnification 10.000x).

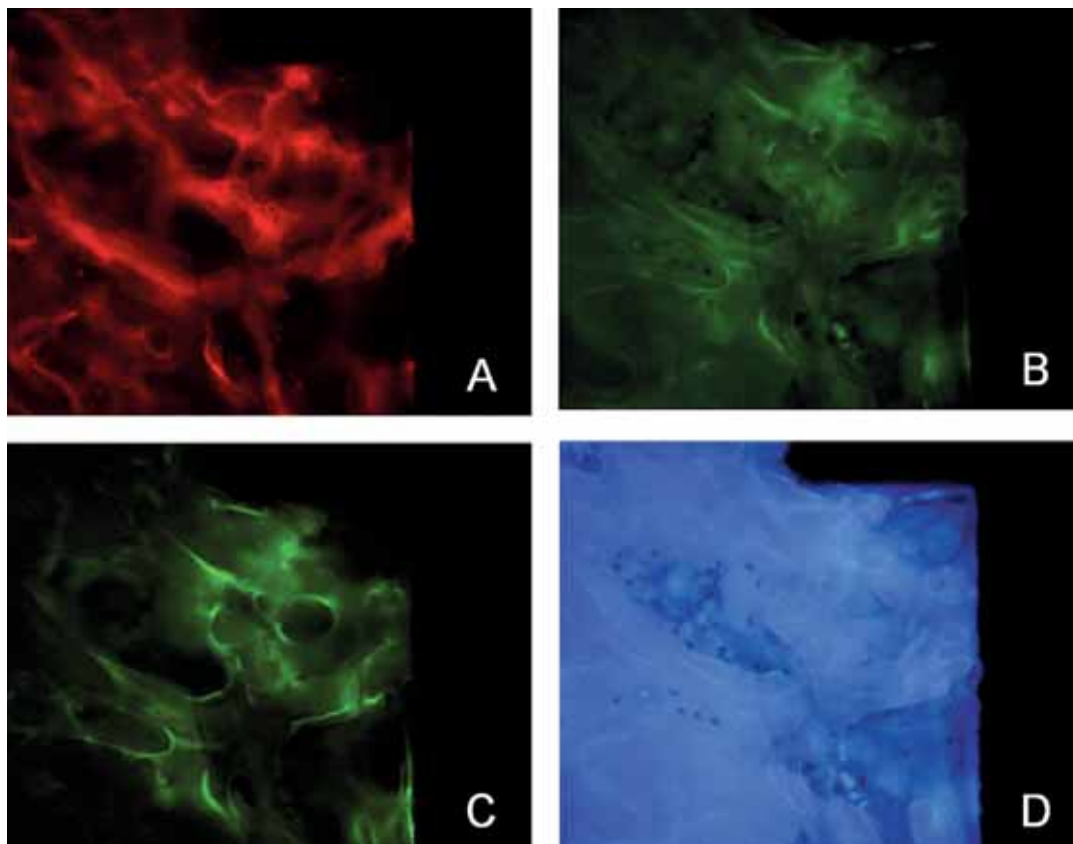


Fig. 3 Fluorescence analysis. New bone formation was determined histomorphometrically by bone markers quantifications inside and outside the indentations. The old bone always appeared darker and without labeling. (A) Alizarin red had a red color in a smeared diffuse pattern; (B) Oxytetracyclin showed thin yellow-green lines; (C) Calcein green was generally represented by clearly evident green bands and (D) Calcein blue was characterized by a blue color in a very diffuse pattern.

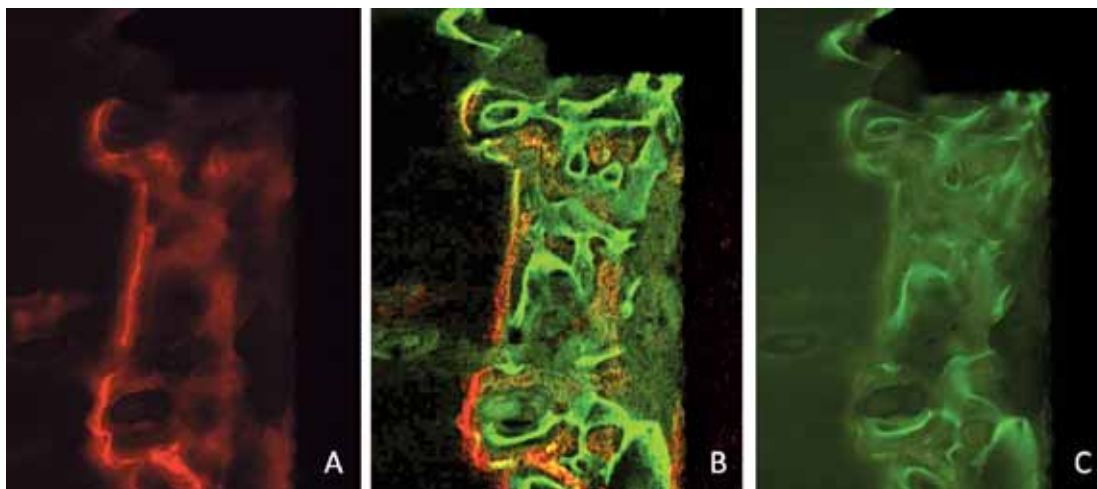


Fig. 4 Fluorescence analysis. (A) Alizarin red; (B) Image obtained from the confocal microscope showing the alizarin red and calcein green together; (C) Calcein green.

Finally, the analysis within the groups that represented the effect of each different surface at the area II (adjacent to the implant surface)

compared to the area OI (distant to the implant surface) demonstrated no statistically significant differences between them.

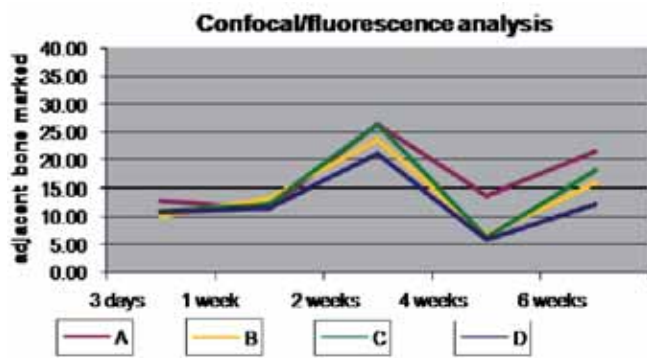


Fig. 5 Graph showing the percentages of newly formed bone inside the indentation (II), adjacent to the implant interface, along the period of evaluation.

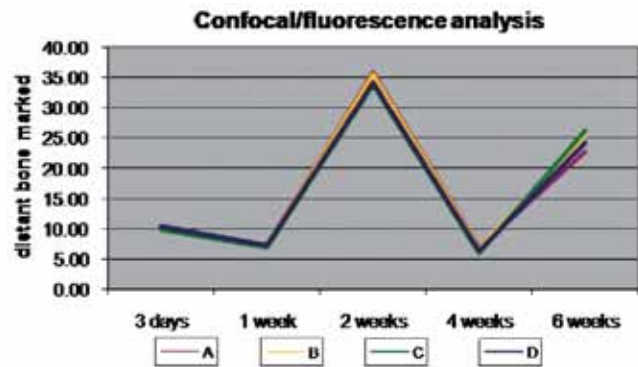


Fig. 6 Graph showing the percentages of newly formed bone outside the indentation (OI), distant to the implant interface, along the period of evaluation.

Adjacent measurements					
Bone marked - Confocal/fluorescence analysis					
	3 days	1 week	2 weeks	4 weeks	6 weeks
A	12.97	11.30	26.41	13.62	21.62
B	10.17	13.20	23.68	6.81	16.07
C	10.89	12.16	26.49	6.39	18.22
D	10.72	11.68	21.19	5.98	12.24

Table 2 The percentages of newly formed bone inside the indentation (II), adjacent to the implant interface, along the period of evaluation.

Distant measurements					
Bone marked - Confocal/fluorescence analysis					
	3 days	1 week	2 weeks	4 weeks	6 weeks
A	10.45	7.21	35.78	6.86	22.73
B	10.38	7.36	35.52	6.72	25.52
C	9.99	7.04	33.84	6.06	26.37
D	10.30	7.17	34.18	6.30	24.14

Table 3 The percentages of newly formed bone outside the indentation (OI), distant to the implant interface, along the period of evaluation.

DISCUSSION

The use of bone markers is essential for fluorescence and CLSM analysis. Their application at different periods permits evaluation of bone formation and remodeling throughout different stages of healing. Alizarin, calcein green, oxytetracyclin and calcein blue fluorochromes present different colors and supply sequential information when applied intercalated. The bone markers used in the present study can be compared because they bind to calcium ions by chelation (15), which allows to properly evidence active mineralization areas (12).

This study evaluated the dynamics of bone formation around different implant surfaces (groups A, B, C and D). Concisely, the fluorochrome incorporation showed a pattern among the different groups of implant surfaces along the period of evaluation from 3 days to 6 weeks. Until the first week, the percentage of marked bone remained between 10 and 13% in all the groups. However at the 2-week evaluation a significant increase in bone formation was detected in all 4 groups. At this moment each group achieved their highest value of marked bone that represented individually their mineralization

peak. At the 4-week evaluation, the level of marked bone decreased considerably for all groups, but for group A in which the decrease was not so pronounced. While groups B, C and D showed their lowest marks at this period, around 6%, group A exhibited 13% of marked bone. Finally at the 6-week period another increase in mineralization activity occurred for all groups (B= 16%, C=18%, D=12%), with slightly better results for group A (21%).

The early phases of bone formation around implants are still poorly understood. Frequently, for example, the studies involving different implant surfaces analyze only the osseointegration determined by the levels of bone-to-implant contact achieved at the end of the experiment. The fluorochrome labeling study makes possible an investigation of the differences in bone formation during the process of bone remodeling, considering 4 or 5 different periods of evaluation. In a different way Abrahamsson et al. (16) evaluated histometrically and morphometrically the healing between 2h and 12 weeks after implant placement in dogs. The dogs were sacrificed and biopsies were obtained in sequential times. From the non-decalcified sections the proportions of woven bone, lamellar bone, non-mineralized structures

(residual tissue) and bone remnants were enumerated and from the decalcified sections the content of osteoblasts, fibroblast-like mesenchymal cells, and mineralized tissue components were distinguished between others.

Taking into account the results obtained in each period of bone remodeling around implants in this study and comparing them to Abrahamsson et al. (16) it was observed that during the first week immediately after implant placement (3- and 7-day periods of evaluation), significant degrees of mineralized components were already found at the area investigated. Bone values ranging from 10 to 13% were achieved for all the groups. According to Abrahamsson et al. (16), at these first steps what could be expected is the presence of a clot becoming partially penetrated by vascular structures surrounded by fibroblast-like mesenchymal cells at its periphery (early granulation tissue), which could not provide substantial matrix mineralization at these premature step. Nevertheless at 1-week, the woven bone formation frequently began and the bone formation centers (primary osteons) were usually recognized (16). At this moment, an increase in mineralized components could be noted, although provisional connective tissue matrix rich in vascular structures was still expected to be present. Abrahamsson et al. (16) described that, in this phase, the primary osteons all consistently were lined by osteoblasts. After 2 weeks the presence of trabeculae of newly formed bone was predictable and occupied the whole architectural space available. At this time an active process of mineralization was present (16). These observations supported the results found in the present study that showed the 2-week period as the mineralization peak for all the groups. In sequence to this ongoing process, at the 4-week period of evaluation a decrease in mineralization levels was observed in the present study, which is explained by the fact that a large volume of woven bone had already been replaced by lamellar bone (16). Subsequently, for the next 4 weeks the formation of secondary osteons and an undergoing remodeling was found. In this process, bone formative and resorptive phases were systematically intercalated and the level of mineralization tended to increase in a slower but gradual way as observed in the 6-week findings of the present study.

Bone remodeling means substitution of bone tissue that improves its quality in both mechanical and metabolic properties (17). Remodeling involves the recruitment of osteoclasts that form a cavity on the trabecular surface. At the end of this resorptive phase, the osteoclasts move on or disappear, and after a short intermission or reversal phase, the osteoblasts start depositing new bone (formative phase) (17). This coupling phenomenon is of special

interest because it involves cells of rather different origin in both cortical and trabecular remodeling units. The initiation of the coupled resorptive and formative activities is obviously based on a concerted action of multiple factors engaged in osteoclast activation, osteoblast proliferation and differentiation, matrix formation, and mineralization. Hence, the superior marked bone found for group A at the 4-week period could be understood as a positive balance for bone formation. It is unknown how the biofunctionalized implant surface with a "low concentration" of peptide of group A may had influenced positively the formative phase favoring significantly the level of mineralization of this group specifically at this period. Considering the mineralization itself, some basic requirements were considered to be absolutely necessary, such as an adequate concentration of calcium and phosphate ions, the presence of calcifiable matrix and nucleating agents, and the control by regulators (ie, promoters and inhibitors) (18).

The bone tissue types could be distinguished by the orientation of the collagen fibrils. In woven bone the collagen fibrils were oriented in a random or feltlike manner while the lamellar bone was characterized by 3- to 5-wide layers of parallel fibrils. Besides, in the fluorochrome labeling analysis the woven bone appeared in a diffuse rather than in a clearly delineated uptake, although the lamellar bone showed well-defined fluorescent bands once the fluorochrome labels were restricted to the mineralization front (17). These patterns for both woven and lamellar bone were observed in the present study. The woven bone was represented by the alizarin red that was administered 1 week after implant placement and exhibited very diffuse labeling. On the other hand the lamellar bone was represented by oxytetracyclin that was administered 2 weeks after implant positioning and also by the calcein green administered at 4 weeks. The images of both fluorochromes showed a clearly different aspect determined by better organized, well-defined fluorescent bands. This finding was in agreement with the bone formation process in bone defects described by Schenk et al. (19) that presumed firstly the establishment of woven bone followed by lamellar bone. The woven bone was formed more rapidly, and the interval between osteoid deposition and mineralization was short. In contrast, lamellar bone formation took place more slowly and mineralization occurred along a clearly delineated front respecting the parallel and/or concentric layers of the collagen fibrils.

It could be concluded that all the implants surfaces studied from the biofunctionalized to the microstructured created by grit-blasting/acid-etching process have a similar pattern in bone remodeling

that could be evidenced by fluorochrome labeling analysis. The biofunctionalized implant surface with an adhesive peptide in "low concentration" favored the bone formation adjacent to the implants when compared to the other surfaces during the period evaluated, which means that different concentrations of bioactive peptide lead to different results.

ACKNOWLEDGEMENTS

This study was supported in part by DENTSPLY Friident and by FAPESP (process numbers 05/60839-8 and 06/56020-6).

REFERENCES

1. Anselme K, Bigerelle M, Noel B, Dufresne E, Judas D, Iost A, Hardouin P. Qualitative and quantitative study of human osteoblast adhesion on materials with various surface roughnesses. *J Biomed Mater Res* 2000;49(2):155-66.
2. MacDonald DE, Markovic B, Allen M, Somasundaran P, Boskey AL. Surface analysis of human plasma fibronectin adsorbed to commercially pure titanium materials. *J Biomed Mater Res* 1998;41:120-30.
3. Rezania A, Healy KE. Biomimetic peptide surfaces that regulate adhesion, spreading, cytoskeletal organization, and mineralization of the matrix deposited by osteoblast-like cells. *Biotechnol Prog* 1999;15:19-32.
4. Rezania A, Thomas CH, Branger AB, Waters CM, Healy KE. The detachment strength and morphology of bone cells contacting materials modified with a peptide sequence found within bone sialoprotein. *J Biomed Res* 1997;37:9-19.
5. Goldberg V, Stevenson S, Feighan J, Davy D. Biology of grit-blasted titanium alloy implants. *Clin Orthop Relat Res* 1995;319:122-9.
6. BBagno A, Piovano A, Dettin M, Chiarion A, Brun P, Gambaretto R, Fontana G, Di Bello C, Palù G, Castagliuolo I. Human osteoblast-like cell adhesion on titanium substrates covalently functionalized with synthetic peptides. *Bone* 2007;40(3):693-9.
7. Schuler M, Owen GR, Hamilton DW, de Wild M, Textor M, Brunette DM, Tosatti SG. Biomimetic modification of titanium dental implant model surfaces using the RGDSP-peptide sequence: a cell morphology study. *Biomaterials* 2006;27(21):4003-15.
8. Park JM, Koak JY, Jang JH, Han CH, Kim SK, Heo SJ. Osseointegration of anodized titanium implants coated with fibroblast growth factor-fibronectin (FGF-FN) fusion protein. *Int J Oral Maxillofac Implants* 2006;21:859-66.
9. Becker J, Kirsch A, Schwarz F, Chatzinikolaïdou M, Rothamel D, Lekovic V, Laub M, Jennissen HP. Bone apposition to titanium implants biocoated with recombinant human bone morphogenetic protein-2 (rhBMP-2). A pilot study in dogs. *Clin Oral Investig* 2006;10(3):217-24.
10. Germanier Y, Tosatti S, Brogginì N, Textor M, Buser D. Enhanced bone apposition around biofunctionalized sandblasted and acid-etched titanium implant surfaces. A histomorphometric study in miniature pigs. *Clin Oral Impl Res* 2006;17:251-7.
11. Suzuki K, Aoki K, Ohya K. Effects of surface roughness of titanium implants on bone remodeling activity of femur in rabbits. *Bone* 1997;21:507-14.
12. Nkenke E, Kloss F, Wiltfang J, Schultze-Mosgau S, Radespiel-Tröger M, Loos K, Neukam FW. Histomorphometric and fluorescence microscopic analysis of bone remodelling after installation of implants using an osteotome technique. *Clin Oral Impl Res* 2002;13(6):595-602.
13. Cho K-S, Choi S-H, Chai J-K, Wikesjö UME, Kim C-K. Alveolar bone formation at dental implant dehiscence defects following guided bone regeneration and xenogenic freeze-dried demineralized bone matrix. *Clin Oral Impl Res* 1998;9:419-28.
14. Donath K, Breuner G. A method for the study of undecalcified bones and teeth with attached soft tissues. The Sage-Schliff (sawing and grinding) technique. *J Oral Pathol* 1982;11:318-26.
15. Sun TC, Mori S, Roper J, Brown C, Hooser T, Burr DB. Do different fluorochrome labels give equivalent histomorphometric information? *Bone* 1992;13:443-6.
16. Abrahamsson I, Berglundh T, Linder E, Lang NP, Lindhe J. Early bone formation adjacent to rough and turned endosseous implant surfaces. An experimental study in the dog. *Clin Oral Impl Res* 2004;15:381-92.
17. Schenk RK. Bone regeneration: biologic basis. In: Buser D, Dahlin C, Schenk RK, eds. *Guided bone regeneration in implant dentistry*. St Louis: Quintessence Publishing Co; 1994. p.49-100.
18. Kahn AJ, Fallon MD, Teitelbaum SL. Structure-function relationships in bone: An examination of events at the cellular level. In: Peck WA, ed. *Bone and mineral research*. Amsterdam: Elsevier; 1983:125-174.
19. Schenk RK, Buser D, Hardwick WR, Dahlin C. Healing pattern of bone regeneration in membrane-protected defects: a histologic study in the canine mandible. *Int J Oral Maxillofac Implants* 1994;9(1):13-29.